

# Time-resolved thermodynamic profiles for CO photolysis from the mixed valence form of bovine heart cytochrome c oxidase†

Randy W. Larsen\*

Received 11th November 2005, Accepted 15th March 2006

First published as an Advance Article on the web 4th April 2006

DOI: 10.1039/b516977a

Photoacoustic calorimetry has been utilized to probe the thermodynamics accompanying photodissociation of the CO mixed valence form of bovine heart cytochrome c oxidase (COMV CcO). At pH's below 9 photolysis of the COMV CcO results in three kinetic phases with the first phase occurring faster than the time resolution of the instrument (*i.e.*,  $< \sim 50$  ns), a second phase occurring with a lifetime of  $\sim 100$  ns and a third phase occurring with a lifetime of  $\sim 2$   $\mu$ s. The corresponding volume and enthalpy changes for these processes are:  $\Delta H_1, \Delta V_1 = +79 \pm 10$  kcal mol<sup>-1</sup>,  $+9 \pm 1$  mL mol<sup>-1</sup>;  $\Delta H_2, \Delta V_2 = -79 \pm 5$  kcal mol<sup>-1</sup>,  $-9 \pm 2$  mL mol<sup>-1</sup>;  $\Delta H_3, \Delta V_3 = +54 \pm 7$  kcal mol<sup>-1</sup>,  $+8 \pm 1$  mL mol<sup>-1</sup>. At pH's above 9 only one phase is observed, a prompt phase occurring in  $< 50$  ns. The overall volume change is negligible above pH 9 and the enthalpy change is  $+29 \pm 5$  kcal mol<sup>-1</sup>. The data are consistent with the prompt phase being associated with CO–Fe<sub>a3</sub> bond cleavage, CO–Cu<sub>B</sub><sup>+</sup> bond formation, Fe<sub>a3</sub> low-spin to high-spin transition and fast electron transfer (ET) from heme *a*<sub>3</sub> to heme *a* followed by proton transfer from Glu242 to Arg38 on an  $\sim 100$  ns timescale. The slow phase is likely a combination of CO thermal dissociation from Cu<sub>B</sub> and additional ET between heme *a*<sub>3</sub> to heme *a*. Interestingly, this phase is not evident above pH 9 suggesting linkage between CO dissociation/ET and the protonation state of a group or groups near the binuclear center.

## Introduction

Heme/copper oxidases form a diverse class of respiratory proteins found in nearly all aerobic organisms.<sup>1–5</sup> Although these enzymes range in molecular weight and subunit composition, several common features are found throughout the class. The majority of heme/copper oxidases contain at least three subunits (SU I, SU II, and SU III) with SU I containing the majority of the redox active metal centers including two heme chromophores (heme *a*, heme *b*, and/or heme *o*) and at least one copper ion (Fig. 1, top). One of the two hemes contains a heme iron that is six-coordinate and low spin which functions as a catalyst for electron transfer (ET) to the binuclear center. The binuclear center consists of the remaining heme (designated heme *a*<sub>3</sub>, heme *o*<sub>3</sub>, or heme *b*<sub>3</sub> depending upon the organism), which contains a five-coordinate high spin heme iron and a copper ion (designated Cu<sub>B</sub>). In addition, heme/copper oxidases from higher organisms contain an additional binuclear copper cluster (designated Cu<sub>A</sub>) which accepts electrons from cytochrome *c*. All members of this class catalyze the four electron reduction of dioxygen to water and it is widely believed that most of these enzymes are energy transducing *i.e.*, they couple redox free energy to the active transport of protons across a membrane.

The overall reduction of dioxygen requires four protons to be consumed from the interior side of the membrane to form two water molecules. During the reduction reaction, four additional

protons are vectorially translocated against a membrane potential from the interior to the exterior side of the membrane. Although the mechanism of active transport in heme/copper oxidases has not yet been fully elucidated, there is now clear experimental evidence that the ET steps within the catalytic cycle are well choreographed with proton uptake and release.<sup>6–11</sup> Studies using site directed mutants as well 3D structural models have now established two proton translocating channels that direct protons to the binuclear center.<sup>6,7</sup> The so-called K-channel begins with Lys319 proceeds through Thr316, Thr309, Ser255, Tyr244 and ends at the binuclear center (bovine heart numbering). The D-channel has an entryway on the cytoplasmic side formed by Asp91 and continues through Asn98 and comes into close proximity of the binuclear center through Glu242. It is believed that the K-channel is active during the first phase of the reaction cycle in which the enzyme accepts two electrons and takes up two protons whereas the D-channel conducts protons to the binuclear center as well as to periplasm during the reduction of various dioxygen intermediates.

Upon input of the first two electrons into the fully oxidized enzyme two protons are taken up from the matrix side of the membrane *via* the K-channel (Fig. 1, bottom) (O to R transitions). At this point, dioxygen binds to the heme *a*<sub>3</sub> group of the binuclear center resulting in heterolytic cleavage of the O–O bond *via* the transfer of four electrons to the bound oxygen (P-state): two electrons being derived from heme *a*<sub>3</sub> (forming a heme *a*<sub>3</sub> oxyferryl intermediate) one electron being derived from Cu<sub>B</sub><sup>+</sup> and one electron from a tyrosine covalently linked to a histidine bound to Cu<sub>B</sub> (forming a tyrosine radical). Subsequent ET from heme *a* (reduced *via* ET from cytochrome *c* to Cu<sub>A</sub> and subsequent ET from Cu<sub>A</sub> to heme *a*) to the oxyferryl heme *a*<sub>3</sub> of the P-state results

Department of Chemistry, University of South Florida, 4202 E. Fowler Ave, Tampa, FL, 33620, USA

† This paper was published as part of the special issue on Proton Transfer in Biological Systems.

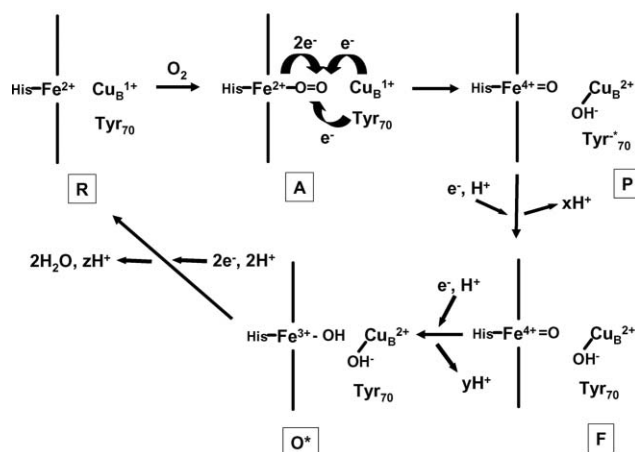
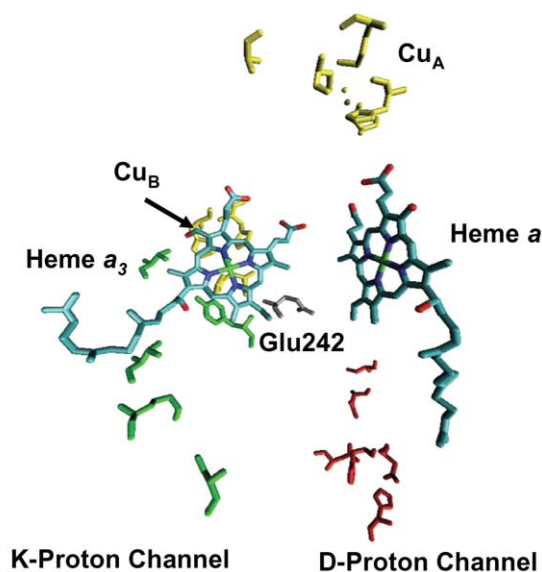


**Fig. 1** Top: Metal center orientation within bovine heart cytochrome c oxidase (CcO). Bottom: Proposed catalytic mechanism for CcO.

in reduction of the tyrosine radical and subsequent proton transfer from Glu242 to either the deprotonated tyrosine or a hydroxide bound to  $\text{Cu}_B$  forming the F-state. Since each electron transferred to the binuclear center appears to be coupled to proton input, an additional proton is taken up during the P to F transition. In addition, at least one proton is also pumped across the membrane at this point in the catalytic cycle. Reduction of the F-state by subsequent ET from cytochrome *c* results in the formation of a hydroxide bound ferric heme  $a_3$ , the input of two protons and the pumping of one additional proton. There is now evidence that electron input from cytochrome *c* to the binuclear center to initiate a new turnover cycle (once the enzyme has completed a full turnover cycle) also results in the pumping of additional protons (O to R transition). The exact mechanism through which protons are actively translocated across the membrane barrier is not clear and a number of models have been proposed.<sup>3,12-15</sup> The most recent models involve electrostatic repulsion between protons within proton loading sites within the enzyme and protons

imported from the input channels upon electron input. In any event, the transfer of electrons is intimately connected with the active transport of protons.

A very useful method to probe the relationship between proton transport and intramolecular ET in heme/copper oxidases involves photolysis of the CO mixed valence derivative of the enzyme.<sup>16-21</sup> In this state, CO is bound to ferrous heme  $x_3$  (where  $x = a, b, \text{ or } o$  depending upon the species) and the  $\text{Cu}_B$  ion is in the +1 state. The remaining metals remain oxidized (heme  $x/\text{Cu}_A$  for cytochrome oxidases, heme  $x$  for quinol oxidases). Photolysis of the CO from the heme  $x_3$  site results in a lowering of the heme  $x_3$  reduction potential allowing for rapid ET between the ferrous heme  $x_3$  and ferric heme  $x$  (Fig. 2). In CcO subsequent ET takes place between heme  $x$  and the cupric  $\text{Cu}_A$  site. The rates of intramolecular ET depend upon the nature of the species from which the enzyme was isolated. Photolysis of CO mixed valence CcO from bovine heart muscle (COMV CcO) results in rapid transfer of CO from heme  $a_3$  to  $\text{Cu}_B$  ( $\sim\text{ps}$ ) followed by rapid ET from heme  $a_3$  to heme  $a$  (1.2 ns).<sup>20,21</sup> Further heme  $a_3$  to heme  $a$  ET occurs on an  $\sim 3 \mu\text{s}$  timescale and it is believed that this ET event is coupled to the thermal release of CO from  $\text{Cu}_B$  since the CO dissociation rate is also  $\sim 3 \mu\text{s}$  in the fully reduced enzyme where heme  $a_3$  to heme  $a$  ET does not occur. Additional ET between heme  $a$  and  $\text{Cu}_A$  occurs on a much longer timescale ( $\sim 75 \mu\text{s}$ ).

#### Mixed Valence

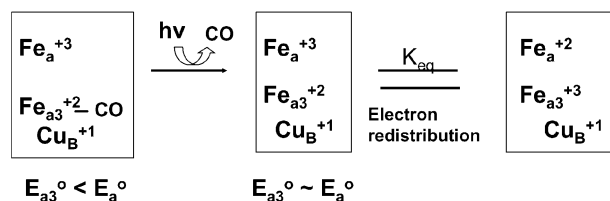


**Fig. 2** Mechanism of intramolecular ET subsequent to photolysis from the COMV form of heme/copper oxidases.

Previous FTIR results of the photostationary state of the COMV CcO have demonstrated pH dependent perturbations.<sup>22,23</sup> It was shown that the photostationary state results in perturbations to Glu242 (attributed to deprotonation of this residue), redox induced shifts in heme propionate vibrational frequencies and redox linked protonation of an Arg residue which appears to accompany ET between heme  $a_3$  and heme  $a$ . These studies could not resolve which ET event was associated with the proton transfer events (*i.e.*, the ns fast phase or the slower phase coupled to thermal release of CO from  $\text{Cu}_B$ ). What is of specific interest is the fact that the protonation state of Glu242 which is located at the end of the D-channel and donates protons to the binuclear center during the P to F transition is directly linked to the redox state of heme  $a$ /heme  $a_3$ .

The obvious relationship between the energetics of ET and the active transport of protons necessitates a complete understanding of the thermodynamics associated with various ET reactions within the enzyme as well as their pH dependence. With this in mind our lab has been utilizing photothermal methods to probe both ET and ligand binding/migration in various forms of heme/copper oxidase from a variety of organisms. In this report, photoacoustic calorimetry (PAC) is utilized to probe the thermodynamics associated with intramolecular ET between heme

$a_3$  and heme  $a$  in the COMV CcO from bovine heart muscle as a function of pH.

## Experimental

Cytochrome c oxidase was purified from bovine heart muscle using a modified Hartzell–Bienert preparation.<sup>24</sup> The enzyme was stored as a stock solution (~350  $\mu\text{M}$ ) in 50 mM HEPES buffer containing 0.05% dodecyl maltoside (DM). Samples were prepared by dilution the stock solution to ~16  $\mu\text{M}$  in 50 mM HEPES buffer containing 0.05% DM (pH 6,8 or 9). The CO mixed valence form of CcO was prepared by de-aerating the sample with Ar for 20 min in a septum sealed 1-cm quartz cuvette. The sample was then purged with CO for 10 minutes followed by room temperature incubation for 1–6 h depending upon solution pH (6 h for pH 6, 1 h for pH 9). Formation of the COMV CcO was verified by UV/VIS spectra obtained using a Shimadzu UV-2401 PC spectrophotometer. Fe(III) (4-sulfonatophenyl) porphine (Fe4SP) (Frontier Scientific Inc.) in 50 mM HEPES buffer, 0.05% DM (pH 6,8 or 9) was used as a calorimetric reference compound for the PAC measurements. Absorbance of the sample and the reference at the excitation wavelength (532 nm) were adjusted to be 0.3.

The instrumentation and application of PAC to study the ET reactions and ligand binding in proteins has been reviewed elsewhere.<sup>25–28</sup> PAC measurements were performed by placing a 1  $\times$  1 cm quartz cuvette containing 1.5 mL of a sample in a temperature controlled sample holder (Quantum Northwest) housing a Panametrics V103 transducer. Contact between the cuvette and the detector was facilitated with a thin layer of vacuum grease. Photo-dissociation of CO was achieved with a 532 nm laser pulse (Continuum Minilite I frequency double Q-switched Nd:YAG laser, 6 ns pulse, <80  $\mu\text{J}$ ). The acoustic signal was amplified with an ultrasonic preamp (Panametrics) and recorded using an NI 5102 Oscilloscope (15 MHz) controlled by VirtualBench software (National Instrument). The PAC data were analyzed using the multiple temperature method in which sample and calorimetric reference acoustic traces are obtained as a function of temperature. The ratio of the amplitudes of the sample and reference acoustic signals ( $\phi$ ) is then plotted *versus*  $C_p\rho/\beta$  according to eqn (1):

$$\phi E_{\text{hv}} = \Phi [Q + \Delta V_{\text{con}}(C_p\rho/\beta)] \quad (1)$$

where  $\phi$  is the ratio of the acoustic amplitude of the sample to that of the reference,  $\Phi$  is the quantum yield (assumed to be one for heme  $a_3$ -CO photolysis),  $Q$  is the heat released to the solvent,  $\beta$  is the coefficient of thermal expansion of the solvent ( $\text{K}^{-1}$ ),  $C_p$  is the heat capacity ( $\text{cal g}^{-1} \text{K}^{-1}$ ),  $\rho$  is the density ( $\text{g mL}^{-1}$ ) and  $\Delta V_{\text{con}}$  represents conformational/electrostriction contributions to the solution volume change. A plot of  $\phi E_{\text{hv}}$  *versus*  $C_p\rho/\beta$  (varied by changing the solution temperature) gives a straight line with a slope equal to  $\Delta V_{\text{con}}$  and an intercept equal to the released heat ( $Q$ ). Subtracting  $Q$  from  $E_{\text{hv}}$  gives  $\Delta H$  for processes occurring faster than the time resolution of the instrument (<50 ns). The  $Q$  values for subsequent kinetic processes represent  $-\Delta H$  for that step (*i.e.*, heat released). However, CcO contains two hemes that can absorb the incident photon. Photons absorbed by heme  $a$  will simply degrade the absorbed photon energy to heat and deposit this energy into the solution within the laser pulse while

photons absorbed by heme  $a_3$  initiate the photolysis reaction. The amount of energy absorbed by each heme depends on their relative absorbance at the excitation wavelength. Using absorption spectra of heme  $a$  model compounds (ferrous heme  $a$  bis-1-methyl imidazole and ferrous heme  $a$  1,2 dimethyl imidazole complexes as models for the heme  $a$  and heme  $a_3$  centers of CcO, respectively) as well as the fact that fully reduced forms of CcO and CO-CcO have equivalent absorbance at 532 nm both hemes contribute nearly equal contributions to the total absorbance at the excitation wavelength of 532 nm. Thus the heat deposited due to the photolysis event at heme  $a_3$  and the corresponding  $\Delta H$ , can be expressed as:

$$Q_{a_3} = 0.5Q_{\text{total}} \quad (2)$$

$$\Delta H = E_{\text{hv}} - Q_{a_3} \quad (3)$$

The acoustic transducer is sensitive to the amplitude of the acoustic waves as well as to their temporal profile, allowing for individual contributions to  $\Delta V_{\text{con}}$  and  $Q$  arising from longer time kinetic events to be resolved. The observed time dependent acoustic signal  $E(t)_{\text{obs}}$  is produced by the convolution of an instrument response function  $T(t)$  (the reference acoustic wave) with a time dependent function of the decay processes,  $H(t)$ :

$$E(t)_{\text{obs}} = H(t) \times T(t) \quad (4)$$

where

$$H(t) = \phi_1 \exp(-t/\tau_1) + [\phi_2 k_1 / (k_2 - k_1)] [\exp(-t/\tau_1) - \exp(-t/\tau_2)] \quad (5)$$

Simplex parameter estimation software developed in our laboratory was used to obtain parameters  $\phi_i$  and  $\tau_i$  (the corresponding rate constants are  $k_i = 1/\tau_i$ ). Processes occurring faster than roughly 50 ns can not be resolved in time but the integrated enthalpy and volume changes can be quantified from the amplitude of the acoustic wave.

## Results and discussion

Fig. 3 displays an overlay of the acoustic traces for the sample and reference obtained at pH 6, pH 8 and pH 9. The acoustic waves obtained at both pH 6 and pH 8 for CO photolysis from the COMV CcO show significant phase shifts relative to those of the corresponding reference compounds. This indicates that enthalpy and/or molar volume changes take place on timescales between the ~50 ns and ~15  $\mu\text{s}$  time window of the PAC instrument. From deconvolution of the sample acoustic waves three kinetic events can be resolved (see Fig. 4). The first occurs faster than the time resolution of the instrument (*i.e.*, <~50 ns), the second has a lifetime of ~100 ns and the third occurs with a lifetime of ~2  $\mu\text{s}$  (at 20  $^\circ\text{C}$ ). Analysis of the temperature dependence of the deconvoluted acoustic amplitudes at pH 6 gives volume and enthalpies associated with the three kinetic phases:  $\Delta H_1$ ,  $\Delta V_1 = +79 \pm 10 \text{ kcal mol}^{-1}$ ,  $+9 \pm 1 \text{ mL mol}^{-1}$ ;  $\Delta H_2$ ,  $\Delta V_2 = -79 \pm 5 \text{ kcal mol}^{-1}$ ,  $-9 \pm 2 \text{ mL mol}^{-1}$ ;  $\Delta H_3$ ,  $\Delta V_3 = +54 \pm 7 \text{ kcal mol}^{-1}$ ,  $+8 \pm 1 \text{ mL mol}^{-1}$  (Fig. 5). Similar volume and enthalpy changes are observed at pH 8. Interestingly, no phase shift is observed at pH 9. Analysis of the amplitudes of the sample and reference acoustic waves obtained at pH 9 reveal no significant volume change (*i.e.*,  $\Delta V \sim 0$ ) and a  $\Delta H$  of  $+29 \text{ kcal mol}^{-1}$ .

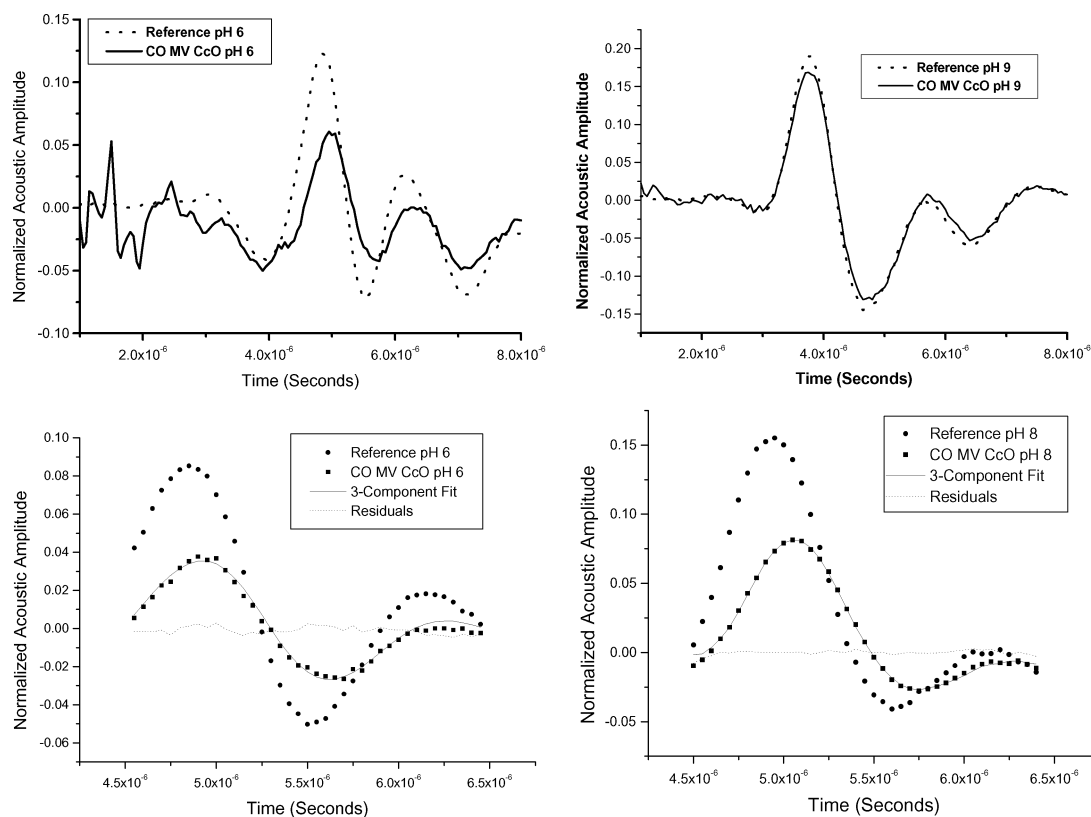


**Fig. 3** Overlay of COMV CcO and calorimetric reference signals obtained at pH 6 (top left), and pH 9 (top right). Sample conditions: [CcO] = 16  $\mu\text{M}$  in 50 mM HEPES buffer containing 0.05%  $\beta\text{-D-laurylmaltoside}$ . Deconvolution of the acoustic waves for COMV CcO showing the three-component fits for pH 6 and 8 are shown in the bottom left and right panels, respectively. Plots show an overlay of acoustic waves for COMV CcO, calorimetric reference, three-exponential fit and residuals.

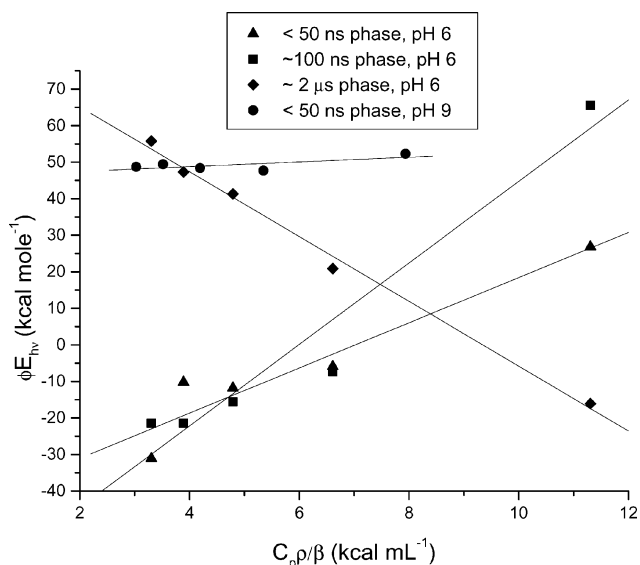


**Fig. 4** Plot of  $\phi E_{iv}$  vs.  $C_p \rho / \beta$  for the acoustic signals obtained at pH extremes, pH 6 and pH 9. The normalized amplitudes ( $\phi_i$ ) for the various phases at pH 6 were obtained from the deconvolution of the acoustic waves as per eqn (4) and (5).

The thermodynamic profiles are summarized in Fig. 5. It is of interest to note that neither the  $\sim 100$  ns nor the  $\sim 2$   $\mu\text{s}$  phase

shows any significant temperature dependence between 10  $^\circ\text{C}$  and 30  $^\circ\text{C}$  suggesting a low activation barrier for each case.

We have previously examined the thermodynamics of CO photodissociation from the fully reduced form of bovine heart CcO as well as *Escherichia coli* cytochrome  $\text{b}_0\text{3}$  (Cbo) using PAC.<sup>19,25,26</sup> The corresponding PAC results for photolysis of bovine heart CO-CcO revealed two exponential decays occurring with lifetimes of  $< 50$  ns and  $\sim 1.7$   $\mu\text{s}$ .<sup>25</sup> The data revealed volume increases of  $\sim +7$   $\text{mL mol}^{-1}$  for both the fast and slow phases, respectively. The corresponding values for  $\Delta H$  were found to be  $+39 \pm 2$   $\text{kcal mol}^{-1}$  and  $+34 \pm 3$   $\text{kcal mol}^{-1}$  for the fast and slow phases, respectively. The two processes observed for CO-CcO photolysis correspond to the transfer of CO from heme  $a_3$  to  $\text{Cu}_B$  ( $< 50$  ns) and the subsequent thermal dissociation of CO from  $\text{Cu}_B$  ( $\sim 1.7$   $\mu\text{s}$ ). The volume changes associated with CO photo-dissociation from heme  $a_3$  and binding to  $\text{Cu}_B$  include Fe-CO bond cleavage, CO- $\text{Cu}_B$  bond formation and a low-spin to high-spin transition at heme  $a_3$ . These changes are expected to contribute  $\sim +10$   $\text{mL mol}^{-1}$  to the overall volume changes occurring  $< 1$  ps (time scale of the CO binding to  $\text{Cu}_B$ ).<sup>29</sup> What is particularly intriguing is the fact that the fast phase observed for the photolysis of CO from CcO gives rise to a volume increase suggesting that the volume change associated with the heme  $a_3$  low-spin to high-spin transition dominates the overall volume change upon CO photolysis. The longer time volume expansion may be attributed to relaxation of the protein upon ligand release from the  $\text{Cu}_B$  site. The volume and enthalpy changes associated with CO photolysis from the fully reduced form

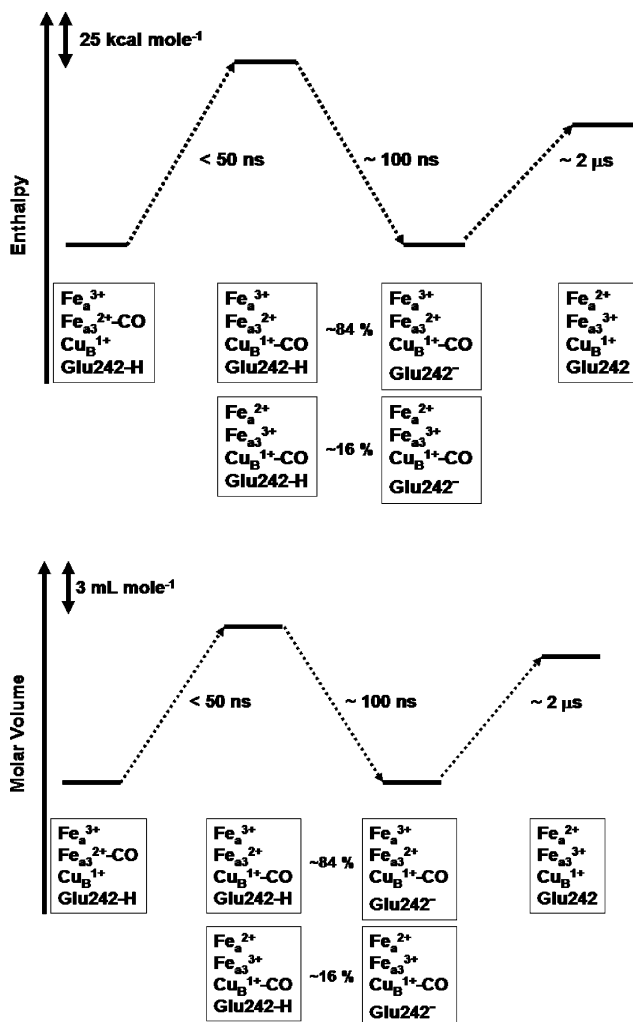


Fig. 5 Thermodynamic profiles (molar volume and enthalpy) for photolysis of COMV CcO at pH's <math>< 9</math>.

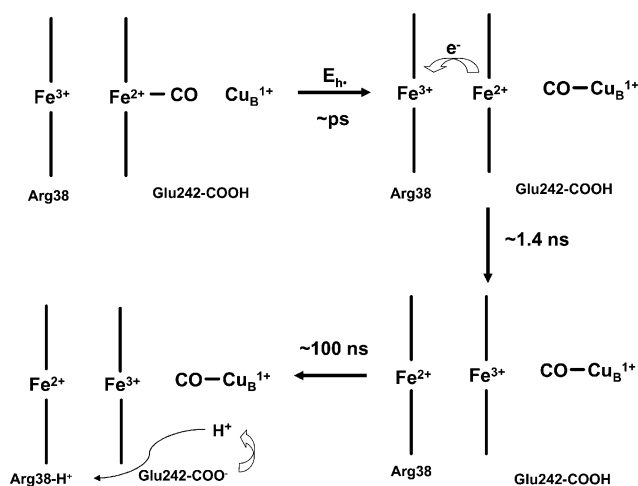


Fig. 6 Proposed mechanism for events occurring subsequent to photolysis of the COMV CcO.

of the enzyme can be utilized in the evaluation of thermodynamic events associated with photolysis of COMV CcO.

### Events occurring in <math>< 50\text{ ns}</math>

The fact that the thermodynamic parameters for processes occurring in <math>< 50\text{ ns}</math> associated with CO photolysis from the COMV CcO are distinct from those obtained for the fully reduced form of the enzyme suggest that additional processes take place in the COMV form of the enzyme. In both the COMV and fully reduced forms of CcO, CO photolysis results in the rupture of the Fe-CO bond, low-spin to high-spin transition and CO-Cu<sub>B</sub> formation. In the case of the COMV form, it has been shown that fast ET takes place with a lifetime of  $\sim 1.2\text{ ns}$ .<sup>21</sup> Thus, the total volume and enthalpy changes for the COMV CcO contain additional parameters associated with the ET between heme *a*<sub>3</sub> and heme *a*:

$$\Delta H_{\text{tot}}^{\text{COMV}} = \Delta H_{\text{Fe-C}}^{\text{COMV}} + \Delta H_{\text{LS-HS}}^{\text{COMV}} + \Delta H_{\text{Cu-C}}^{\text{COMV}} + \Delta H_{\text{ET}}^{\text{COMV}} \quad (6)$$

$$\Delta V_{\text{tot}}^{\text{COMV}} = \Delta V_{\text{Fe-C}}^{\text{COMV}} + \Delta V_{\text{LS-HS}}^{\text{COMV}} + \Delta V_{\text{Cu-C}}^{\text{COMV}} + \Delta V_{\text{ET}}^{\text{COMV}} \quad (7)$$

The thermodynamic events associated with the fast ET can be directly obtained using the parameters obtained from the fully reduced enzyme since:

$$\Delta H_{\text{tot}}^{\text{CO-CcO}} = \Delta H_{\text{Fe-C}}^{\text{CO-CcO}} + \Delta H_{\text{LS-HS}}^{\text{CO-CcO}} + \Delta H_{\text{Cu-CO}}^{\text{CO-CcO}} \quad (8)$$

$$\Delta V_{\text{tot}}^{\text{CO-CcO}} = \Delta V_{\text{Fe-C}}^{\text{CO-CcO}} + \Delta V_{\text{LS-HS}}^{\text{CO-CcO}} + \Delta V_{\text{Cu-CO}}^{\text{CO-CcO}} \quad (9)$$

Thus,

$$\Delta H_{\text{ET}}^{\text{COMV}} = \Delta H_{\text{tot}}^{\text{COMV}} - \Delta H_{\text{tot}}^{\text{CO-CcO}} \quad (10)$$

$$\Delta V_{\text{ET}}^{\text{COMV}} = \Delta V_{\text{tot}}^{\text{COMV}} - \Delta V_{\text{tot}}^{\text{CO-CcO}} \quad (11)$$

From eqn (10) and (11) the average thermodynamic parameters associated with heme *a*<sub>3</sub> to heme *a* ET at pH's below 9 are:  $\Delta H_{\text{ET}}^{\text{COMV}} = +40\text{ kcal mol}^{-1}$  and  $\Delta V_{\text{ET}}^{\text{COMV}} = +2\text{ mL mol}^{-1}$ . These thermodynamic parameters are nearly equivalent between pH 6 and pH 8. Previous studies have suggested that the ultra-fast ET (occurring on the 1.2 ns time scale) accounts for only  $\sim 16\%$  of the total heme *a*<sub>3</sub> to heme *a* ET.<sup>16,21</sup> Scaling  $\Delta H_{\text{ET}}^{\text{COMV}} = +40\text{ kcal mol}^{-1}$  and  $\Delta V_{\text{ET}}^{\text{COMV}} = +2\text{ mL mol}^{-1}$  to the ET yield gives 250 kcal mol<sup>-1</sup> and 12.5 mL mol<sup>-1</sup> for the reaction. The magnitude of the enthalpy value suggests that additional conformational processes must occur in the COMV form of the enzyme, possibly accompanying the ultra-fast ET, which would contribute to the  $\Delta H_{\text{ET}}^{\text{COMV}}$  term (*i.e.*,  $\Delta H_{\text{ET}}^{\text{COMV}} = \Delta H_{\text{ET-effective}}^{\text{COMV}} + \Delta H_{\text{conf}}^{\text{COMV}}$ ). Estimates of the values of these enthalpies can be made using the  $\sim 2\ \mu\text{s}$  data discussed below. What is notable is that the PAC results indicate both fast ET as well as a corresponding reorganization of the heme *a*<sub>3</sub>/Cu<sub>B</sub> active site that may be coupled to the ET reaction.

### Events occurring with a lifetime of $\sim 2\ \mu\text{s}$

In fully reduced CO-CcO photolysis results in the rapid transfer of CO from heme *a*<sub>3</sub> to Cu<sub>B</sub> within a few ps. Subsequent thermal dissociation of CO from the Cu<sub>B</sub> site occurs with a lifetime of  $\sim 1.7\ \mu\text{s}$ .<sup>30,31</sup> Interestingly, thermal dissociation of CO from Cu<sub>B</sub> does not result in CO rebinding to heme *a*<sub>3</sub> which might be expected due to the close proximity of the two metal centers (4.5 Å). Thus, CO binding to Cu<sub>B</sub><sup>+</sup> must trigger a conformational rearrangement

at the Cu<sub>B</sub>/heme *a*<sub>3</sub> site that significantly increases the energy barrier for heme *a*<sub>3</sub> ligand binding while lowering the barrier for CO diffusion out of the active site pocket. Our previous PAC studies have shown that thermal dissociation from Cu<sub>B</sub><sup>+</sup> gives rise to  $\Delta H_{\text{Cu-CO}} = +34 \text{ kcal mol}^{-1}$  and  $\Delta V_{\text{Cu-CO}} = +7 \text{ mL mol}^{-1}$ .<sup>25</sup> In the case of the COMV CcO previous results have also suggested that intramolecular ET also occurs between heme *a*<sub>3</sub> and heme *a* that is coupled to CO release from Cu<sub>B</sub><sup>+</sup>,<sup>16–18,20,21</sup> The slow phase kinetics observed subsequent to photolysis of the COMV CcO presumably contains thermodynamic parameters for both the thermal dissociation of CO as well as any intramolecular ET between the two hemes. Assuming that the Cu<sub>B</sub><sup>+</sup>–CO bond energy is the same in both the COMV and fully reduced forms of the enzyme then the thermodynamic parameters associated with intramolecular ET can also be calculated using:

$$\Delta H_{\text{tot,slow}}^{\text{CO-CcO}} = \Delta H_{\text{Cu-CO}}^{\text{CO-CcO}} + \Delta H_{\text{Conf}}^{\text{CO-CcO}} \quad (12)$$

$$\Delta V_{\text{tot,slow}}^{\text{CO-CcO}} = \Delta V_{\text{Cu-CO}}^{\text{CO-CcO}} + \Delta V_{\text{Conf}}^{\text{CO-CcO}} \quad (13)$$

and,

$$\Delta H_{\text{tot,slow}}^{\text{COMV}} = \Delta H_{\text{Cu-C}}^{\text{COMV}} + \Delta H_{\text{ET}}^{\text{COMV}} + \Delta H_{\text{Conf}} \quad (14)$$

$$\Delta V_{\text{tot,slow}}^{\text{COMV}} = \Delta V_{\text{Cu-C}}^{\text{COMV}} + \Delta V_{\text{ET}}^{\text{COMV}} + \Delta V_{\text{Conf}} \quad (15)$$

Using eqn (12)–(15) the volume and enthalpy changes associated with the intramolecular ET can be calculated. At pH's below 9 the thermodynamic parameters are:  $\Delta H_{\text{ET}}^{\text{COMV}} \sim 20 \text{ kcal mol}^{-1}$  and  $\Delta V_{\text{ET}}^{\text{COMV}} \sim 1 \text{ mL mol}^{-1}$ . This also assumes that  $\Delta H_{\text{Conf}}$  and  $\Delta V_{\text{Conf}}$  are also equivalent between the COMV CcO and CO-CcO. If the observed  $\Delta H_{\text{ET}}^{\text{COMV}}$  is  $20 \text{ kcal mol}^{-1}$  and this enthalpy represents 86% of the total ET then the actual enthalpy change for the ET reaction is  $\Delta H_{\text{ET}}^{\text{COMV}}/0.86$  or  $+23 \text{ kcal mol}^{-1}$ . Using this value gives  $\Delta H_{\text{ET-conf}}^{\text{COMV}}$  observed in the fast phase to be  $(+40 \text{ kcal mol}^{-1} - (23 \text{ kcal mol}^{-1} \times 0.16)) = +36 \text{ kcal mol}^{-1}$ . The 0.16 scaling factor is used since only 16% of the total ET occurs in the fast phase. The observed volume change is also quite small for the ET reaction which is consistent with no additional conformational change taking place. The ET reaction itself results in no net change in charge ( $\text{Fe}_a^{3+} \text{Fe}_{a3}^{2+} \rightarrow \text{Fe}_a^{2+} \text{Fe}_{a3}^{3+}$ ) therefore no electrostriction would occur and  $\Delta V$  would be negligible.

### Events occurring with a lifetime of ~100 ns

The origin of the ~100 ns phase is not clear. It is not observed in the fully reduced form of the enzyme nor has such a phase been identified in previous transient absorption studies on this time scale. The current hypothesis is that the ~100 ns phase represents either a change in the protonation state of Glu242 or a conformational perturbation to this residue or both. Previous FTIR studies of the mixed valence form of bovine CcO have shown that reverse ET from heme *a*<sub>3</sub> to heme *a* is accompanied by deprotonation of Glu242.<sup>33</sup> This is evident by the appearance of a trough at  $1735 \text{ cm}^{-1}$  in the photolyzed minus unphotolyzed CO mixed valence difference spectrum (arising from Glu242  $\nu_{\text{C=O}}$ ).<sup>22,32</sup> A corresponding carboxylate peak is also observed at  $1412 \text{ cm}^{-1}$ . The nature of the subsequent proton acceptor has not been identified but a putative mechanism involves protonation of an Arg residue near the formyl group of heme *a*. The same FTIR studies have revealed vibrational stretches consistent with protonation

of a neutral Arg (vibrational features at  $1638/1676 \text{ cm}^{-1}$  in the photolyzed/unphotolyzed COMV difference spectrum). The Arg residues near the heme propionates (Arg438 and Arg439) have been ruled out since these residues are located in a hydrophilic region of the protein making it unlikely that any significant population of the deprotonated state would exist. An alternative assignment involves protonation of Arg38 which forms a hydrogen bond with the formyl group of heme *a* since Arg38 is in a more hydrophobic region of the binuclear center (see Fig. 6)

The thermodynamics associated with this phase ( $\Delta H_2, \Delta V_2 = -79 \pm 5 \text{ kcal mol}^{-1}, -9 \pm 2 \text{ mL mol}^{-1}$ ) are consistent with deprotonation. The observed volume contraction could result from significant electrostriction produced within the enzyme by the redistribution of charge (*i.e.*, deprotonation of Glu242 and protonation of the neutral Arg38). In fact, charge separation in bacterial photosynthetic reaction centers from *Rhodobacter sphaeroides* as well as photosystem I (PSI) from *Synechocystis* exhibit volume contractions on the order of  $-9$  to  $-16 \text{ mL mol}^{-1}$  upon charge transfer (*i.e.*,  $\text{P}_{870}^+ \text{Q}_A^-$  formation in bacterial reaction centers and  $\text{P}_{700}^+ \text{F}_{AB}^-$  formation in PSI).<sup>34</sup> Typical values for electrostriction for charge formation in water are in the  $-15 \text{ mL mol}^{-1}$  and the lower value in CcO may reflect a lower dielectric constant within the binuclear center. The enthalpy for proton transfer is more difficult to interpret. Previous studies of the photocycle of bacteriorhodopsin have revealed that proton transfer from Asp96 to the retinal Schiff base ( $\text{M}_2$  to  $\text{N}$  transition) has an associated change in enthalpy of only  $\sim -5 \text{ kcal mol}^{-1}$  whereas the  $\text{N}$  to  $\text{O}$ , which involves proton transfer from Asp85 to the 'release' group near the surface of the protein has an associated enthalpy change of  $\sim -20 \text{ kcal mol}^{-1}$ .<sup>35,36</sup> These enthalpies are considerably higher than the  $\sim -80 \text{ kcal mol}^{-1}$  observed for the 100 ns phase in the COMV CcO. It should be kept in mind that the enthalpy changes observed for proton transfer reactions in the bacteriorhodopsin photocycle also involve significant conformational changes which are also included in the enthalpy changes. Thus, the intrinsic proton transfer enthalpies cannot be isolated from the total enthalpy changes. In the case of CcO it is possible that the larger enthalpy values may represent only the proton transfer event. In fact, gas phase proton transfer reactions exhibit enthalpy changes which are much closer to the CcO values.<sup>37,38</sup>

### pH Dependence

The assignment of the ~100 ns phase to a proton transfer from Glu242 to Arg38 is supported, to some extent, by the fact that this phase is not present at pH's above 9 in which the Glu242 is likely to be deprotonated. It is also of interest that the  $\mu\text{s}$  phase is also absent at higher solution pH values. The pH dependence of this phase suggests that both thermal dissociation of CO from the Cu<sub>B</sub><sup>+</sup> site and corresponding ET from heme *a*<sub>3</sub> to heme *a* may be influenced by the protonation state of Glu242. Interestingly, transient absorption studies by Verkhovsky *et al.*<sup>20</sup> indicate that the lifetime of the  $2 \mu\text{s}$  phase is not pH dependent. Thus, the lack of enthalpy/volume changes in the PAC on this timescale suggests that  $\Delta V$  and/or  $\Delta H$  may be significantly smaller at higher pH. This would suggest that the thermodynamics of thermally activated CO dissociation from Cu<sub>B</sub><sup>+</sup> are coupled to the protonation state of Glu242. Thus, Glu242 may play a role in the modulation of the Cu<sub>B</sub> ligand environment.

**Table 1** Summary of molar volume and enthalpy changes subsequent to photolysis of CO from mixed valence and fully reduced forms of bovine heart cytochrome c oxidase. Enthalpy values are in kcal mol<sup>-1</sup> and molar volume changes are in mL mol<sup>-1</sup>

Sample	$\Delta H_1$ (<50 ns)	$\Delta V_1$ (<50 ns)	$\tau_2$ /ns	$\Delta H_2$	$\Delta V_2$	$\tau_3$ / $\mu$ s	$\Delta H_3$	$\Delta V_3$
COMV CcO, pH 6	+75 $\pm$ 7	+6 $\pm$ 1	70	-82 $\pm$ 2	-9 $\pm$ 0.4	2.5	+66 $\pm$ 11	+11 $\pm$ 2
COMV CcO, pH 8	+83 $\pm$ 12	+11 $\pm$ 2	100	-76 $\pm$ 8	-8 $\pm$ 3	2.5	+41 $\pm$ 10	+4 $\pm$ 2
COMV CcO, pH 9	+29 $\pm$ 5	0	—	—	—	—	—	—
CO-FRCCo	+39 $\pm$ 2	+7 $\pm$ 2	—	—	—	1.7	+34 $\pm$ 3	+7 $\pm$ 2

## Conclusions

The results presented here demonstrate pH dependent thermodynamics associated with ET between the heme groups in COMV CcO and suggest a possible role for Glu242 in both proton transfer within the binuclear center as well as in gating thermal release of CO from the active site. Although the phase observed in  $\sim$ 100 ns can only be tentatively assigned to a proton transfer event it is the first observation of a thermodynamic process in the COMV form of CcO occurring on this timescale. The thermodynamic profiles presented here also represent the first direct measurement of the ET energetics of the fast ET events in CcO.

## Abbreviations

PAC, photoacoustic calorimetry; HEPES, 1-piperazineethane sulfonic acid, 4-(2-hydroxyethyl)-monosodium salt; Fe4SP, Fe(3+)tetrakis (4-sulfonatophenyl) porphyrin; COMV CcO, CO mixed valence cytochrome c oxidase; ET, electron transfer; Cbo, *E. coli* cytochrome bo<sub>3</sub>.

## Acknowledgements

The author would like to thank Prof. Jaroslava Miksovská, Marshall University, for helpful discussions during this work. He would also like to acknowledge the American Heart Association (AHA 025537), the National Science Foundation (NSF MCB0317334) and the Petroleum Research Fund from the American Chemical Society (43423-AC4) for support of these studies.

## References

- 1 R. B. Gennis, Coupled Proton and ET Reactions in Cytochrome c Oxidase, *Front. Biosci.*, 2004, **9**, 581–591.
- 2 K. Faxen, G. Gilderson, P. Adelroth and P. Brzezinski, A Mechanistic Principle for Proton Pumping by Cytochrome c Oxidase, *Nature*, 2005, **437**, 286–289.
- 3 S. Papa, Role of Cooperative H<sup>+</sup>/e<sup>-</sup> Linkage (Redox Bore Effect) at Heme a/Cu<sub>A</sub> and Heme a<sub>3</sub>/Cu<sub>B</sub> in the Proton Pump of Cytochrome c Oxidase, *Biochemistry (Moscow)*, 2005, **70/2**, 220–230.
- 4 D. Bloch, I. Belevich, A. Jasaitis, C. Ribacka, A. Puustinen, M. I. Verkhovskiy and M. Wikstrom, The Catalytic Cycle of Cytochrome c Oxidase is not the sum of its Two Halves, *Proc. Natl. Acad. Sci. USA*, 2004, **101**, 529–533.
- 5 A. Namslauer, A. S. Pawate, R. B. Gennis and P. Brzezinski, Redox-coupled proton translocation in biological systems: Proton shuttling in cytochrome c oxidase, *Proc. Natl. Acad. Sci. USA*, 2003, **100**, 15543–15547.
- 6 M. Wikstrom, A. Jasaitis, C. Backgren, A. Puustinen and M. I. Verkhovskiy, The Role of the K- and D-Pathways of Proton Transfer in the Function of the Haem-Copper Oxidases, *Biochim. Biophys. Acta*, 2000, **1459**, 514–520.

- 7 A. A. Konstantinov, S. Siletsky, D. Mitchell, A. Kaulen, A. and R. B. Gennis, The Roles of the Two Proton Input Channels in Cytochrome c Oxidase from *Rhodobacter sphaeroides* Probed by the Effects of Site-Directed Mutations on Time-Resolved Electrogenic Intraprotein Proton Transfer, *Proc. Natl. Acad. Sci. USA*, 1997, **94**, 9085–9090.
- 8 M. Olivberg, S. Hallen and T. Nilsson, Uptake and Release of Protons During the Reaction between Cytochrome Oxidase and Molecular Oxygen, *Biochemistry*, 1991, **30**, 436–440.
- 9 D. Zaslavsky, A. D. Kaulen, I. A. Smirnova, T. Vygodina and A. A. Konstantinov, Flash-Induced Membrane Potential Generation by Cytochrome c Oxidases, *FEBS Lett.*, 1993, **336**, 389–393.
- 10 M. I. Verkhovskiy, J. E. Morgan, M. L. Verkhovskiy and M. Wikstrom, Translocation of Electric Charge During a Single Turnover of Cytochrome c Oxidase, *Biochim. Biophys. Acta*, 1997, **1318**, 6–10.
- 11 M. Karpefors, P. Adelroth, Y. Zhen, S. Ferguson-Miller and P. Brzezinski, Proton Uptake Controls ET in Cytochrome c Oxidase, *Proc. Natl. Acad. Sci. USA*, 1998, **95**, 13606–13611.
- 12 H. Michel, The Mechanism of Proton Pumping by Cytochrome c Oxidase, *Proc. Natl. Acad. Sci. USA*, 1998, **95**, 12819–12824.
- 13 M. Wikstrom, M. I. Verkhovskiy and G. Hummer, Water Gated Mechanism of Proton Translocation by Cytochrome c Oxidase, *Biochim. Biophys. Acta*, 2003, **1604**, 61–65.
- 14 D. M. Popovic and A. A. Stuchebrukhov, A Proton Pumping Mechanism and Catalytic Cycle of Cytochrome c Oxidase: Coulomb Pump Model with Kinetic Gating, *FEBS Lett.*, 2004, **566**, 126–130.
- 15 P. Brzezinski and G. Larsson, Redox-Driven Proton Pumping by Heme-Copper Oxidases, *Biochim. Biophys. Acta*, 2003, **1605**, 1–13.
- 16 P. Adelroth, P. Brzezinski and B. G. Malmström, Internal ET in cytochrome c oxidase from *Rhodobacter sphaeroides*, *Biochemistry*, 1995, **34**, 2844–2849.
- 17 A. Namslauer, M. Branden and P. Brzezinski, The rate of internal heme-heme ET in cytochrome C oxidase, *Biochemistry*, 2002, **41**, 10369–74.
- 18 J. E. Morgan, P. M. Li, D. Jang, M. A. El-Sayed and S. I. Chan, ET between cytochrome a and copper A in cytochrome c oxidase: a perturbed equilibrium study, *Biochemistry*, 1989, **28**, 6975–83.
- 19 J. Miksovská, R. B. Gennis and R. W. Larsen, Volume and Enthalpy Changes Associated with Intramolecular ET in *Escherichia coli* Cytochrome bo<sub>3</sub>, *FEBS Lett.*, 2005, **579**, 3014–3018.
- 20 M. I. Verkhovskiy, A. Jasaitis and M. Wikstrom, Ultrafast haem-haem ET in cytochrome c oxidase, *Biochim. Biophys. Acta*, 2001, **1506**, 143–6.
- 21 E. Pilet, A. Jasaitis, U. Liebel and M. H. Vos, ET between Hemes in Mammalian Cytochrome c Oxidase, *Proc. Natl. Acad. Sci. USA*, 2004, **101**, 16198–16203.
- 22 B. H. McMahon, M. Fabian, F. Tomson, T. P. Causgrove, J. A. Bailey, F. N. Rein, R. B. Dyer, G. Palmer, R. B. Gennis and W. H. Woodruff, FTIR Studies of Internal Proton Transfer Reactions Linked to Inter-Heme ET in Bovine Cytochrome c Oxidase, *Biochim. Biophys. Acta*, 2004, **1655**, 321–331.
- 23 P. Hellwig, B. Rost and W. Mantele, Redox Dependent Conformational Changes in the Mixed Valence form of the Cytochrome c Oxidase from *P. denitrificans* The Reorganization of Glutamic Acid 278 is Coupled to the ET from/to Heme a and the Binuclear Center, *Spectrochim. Acta, Part A*, 2001, **57A**, 1123–1131.
- 24 C. R. Hartzell and H. Beinert, Components of cytochrome c oxidase detectable by EPR spectroscopy, *Biochim. Biophys. Acta*, 1974, **368**, 318–334.
- 25 R. W. Larsen and T. Langley, Volume Changes Associated with CO-Photolysis from Fully Reduced Bovine Heart Cytochrome aa<sub>3</sub>, *J. Am. Chem. Soc.*, 1999, **121**, 4495–4499.
- 26 R. W. Larsen, J. Osborne, T. Langley and R. B. Gennis, Volume Changes upon Photolysis of Fully Reduced CO-bound Cytochrome bo<sub>3</sub> from *Escherichia coli*, *J. Am. Chem. Soc.*, 1998, **120**, 8887–8888.

- 
- 27 J. Miksovská and R. W. Larsen, Structure–function relationships in metalloproteins, *Methods Enzymol.*, 2003, **360**, 302–329.
- 28 S. E. Braslavsky and G. E. Heibel, Time-resolved photothermal and photoacoustic methods applied to photoinduced processes in solution, *Chem. Rev.*, 1992, **92**, 1381–410.
- 29 R. van Eldik, A. Asano and W. J. le Noble, Activation and Reaction Volumes in Solution, *Chem. Rev.*, 1989, **89**, 549.
- 30 D. D. Lemon, M. W. Calhoun, R. B. Gennis and W. H. Woodruff, The Gateway to the Active Site of Heme-Copper Oxidases, *Biochemistry*, 1993, **32**, 11953–11956.
- 31 O. Einarsdóttir, B. R. Dyer, D. D. Lemon, P. M. Killough, S. M. Hubig, S. J. Atherton, J. J. Lopez-Garriga, G. Palmer and W. H. Woodruff, Photodissociation and Recombination of Carbonmonoxy Cytochrome Oxidase: Dynamics from Picoseconds to Kiloseconds, *Biochemistry*, 1993, **32**, 12013–12024.
- 32 M. Ralle, M. L. Verkhovskaya, J. E. Morgan, M. I. Verkovsky, M. Wikström and N. J. Blackburn, Coordination of Cu<sub>B</sub> in Reduced and CO-Ligated States of Cytochrome bo<sub>3</sub> from *Escherichia coli*. Is Chloride Ion a Cofactor?, *Biochemistry*, 1999, **38**, 7185–7194.
- 33 D. Heitbrink, H. Sigurdson, C. Bolwien, P. Brzezinski and J. Heberle, Transient Binding of CO to Cu<sub>B</sub> in Cytochrome c Oxidase is Dynamically Linked to Structural Changes around a Carboxyl Group: A Time Resolved Step-Scan Fourier Transform Infra-red Investigation, *Biophys. J.*, 2002, **82**, 1–10.
- 34 D. Mauzerall, J.-M. Hou and V. A. Boichenko, Volume Changes and Electrostriction in the Primary Photoreactions of Various Photosynthetic Systems: Estimation of Dielectric Coefficient in Bacterial Reaction Centers and the Observed Volume Changes with the Drude–Nernst Equation, *Photosynth. Res.*, 2002, **74**, 173–180.
- 35 K. Ludmann, C. Gergely and G. Varo, Kinetic and Thermodynamic Study of the Bacteriorhodopsin Photocycle Over a Wide pH Range, *Biophys. J.*, 1998, **75**, 3110–3119.
- 36 A. Onufriev, A. Smondyrev and D. Bashford, Proton Affinity Changes Driving Unidirectional Proton Transport in the Bacteriorhodopsin Photocycle, *J. Mol. Biol.*, 2003, **332**, 1183–1193.
- 37 M. J. S. Dewar and K. M. Dieter, Evaluation of AM1 Calculated Proton Affinities and Deprotonation Enthalpies, *J. Am. Chem. Soc.*, 1986, **108**, 8075–8086.
- 38 Z. B. Maksic and B. Kovacevic, Towards the Absolute Proton Affinities of 20  $\alpha$ -Amino Acids, *Chem. Phys. Lett.*, 1999, **307**, 497–504.